

# Optical absorption engineering in dispersive band structure of MWCNTs array: design and optimization of total absorber for NIR to MIR regime

Bitā Etemadi<sup>1</sup> and Alireza Mobini<sup>2,\*</sup>

1. Department of Electrical and Computer Engineering, Qom University of Technology, Qom, Iran

2. Department of Electrical and Computer Engineering, Islamic Azad University Tehran North Branch, Tehran, Iran

(Received 9 February 2022; Revised 9 May 2022)

©Tianjin University of Technology 2022

In this paper, we design a total infrared (IR) absorber based on a dispersive band structure of two-dimensional (2D) multiwall carbon nanotube (MWCNTs) square array working from near IR (NIR) to mid IR (MIR) regime. The absorption characteristics have been investigated by the 2D finite-difference time domain (FDTD) method in square lattice photonic crystal (PC) of the multipole Drude-Lorentz model inserted to the dispersive dielectric function of MWCNTs. Dispersive photonic band structure and scattering parameters for the wide range of lattice constants from 15 nm to 3 500 nm with various filling ratios have been calculated. The results show that for large lattice constant (>2 000 nm), the Bragg gap moves to the IR regime and leads to MWCNTs arrays acting as a total absorber. For a structure with lattice constant of 3 500 nm and filling factor of 12%, an enhanced absorption coefficient up to 99% is achieved in the range of 0.35 eV ( $\lambda=3.5 \mu\text{m}$ ) nominated in the MIR regime. Also, the absorption spectrum peak can be tuned in the range of 0.27–0.38 eV ( $\lambda=4.59\text{—}3.26 \mu\text{m}$ ) with a changing filling factor. Our results and methodology can be used to design new MWCNTs based photonic devices for applications like night-vision, thermal detector, and total IR absorbers.

**Document code:** A **Article ID:** 1673-1905(2022)09-0513-6

**DOI** <https://doi.org/10.1007/s11801-022-2018-5>

Carbon nanotubes (CNTs), which are famous in nanotechnology field, were first discovered by IJIMA in 1991. In fact reporting the fullerene by SMALLEY and his colleagues boosted his morale to think of new carbon structure and expectantly led to new carbon allotropic termed CNT<sup>[1-3]</sup>. In stable condition, this material is categorized in single-wall and multiwall types. Single-wall CNTs (SWCNTs) are produced by rolling up the graphene sheet. Depending on the rolling sheet orientation, it can be conductor or semiconductor. Besides, multiwall CNTs (MWCNTs) are rolled up graphite sheets<sup>[4]</sup>. It is worth to note that bonding between the atoms in each hollow cylinder is covalent force, while the bonding among the atoms of the collapsed cylinders is of the van der Waals force<sup>[5]</sup>.

As long as CNTs can pass the electric current through the surface without the friction of an electron, they are an ideal choice for many microelectronic applications<sup>[2,3,6,7]</sup>. These nanostructures, due to their exclusive mechanical, electrical, chemical, and magnetic properties, possibly will be used in electronics, hydrogen storage, transistors, batteries, sensors, memories,

screens, power cables and so on<sup>[2,3,8-13]</sup>. Advanced utilities of CNTs led them to appear in various hypothetical and empirical researches, including photonic crystal (PC) structure<sup>[14]</sup>.

PCs are the structures whose refractive index alters intermittently<sup>[15,16]</sup>. The function of PCs against photons is similar to the function of semiconductor crystals (structures with intermittent electrical potential) against electrons<sup>[17]</sup>. The wavelengths of light which are allowed to propagate along the structure are labelled as “modes”. On the other hand, prohibited bands of PCs are denominated as photonic band gaps (PBGs) which caused intense scattering of electromagnetic waves (Bragg scattering). As a matter of fact, the main attribute of PCs is the attendance of PBGs<sup>[17,18]</sup>. Perpendicular aligned periodic array of MWCNTs with explicit dimensions comparable to light wavelength results in marvelous PBGs comprising the plasmonic bands of graphite<sup>[10,19]</sup>. The nonlinearity and anisotropy of CNT materials are tremendously approved<sup>[20-22]</sup>. However, they seem to have resembling intimacy with graphite. The approaching light in transverse-magnetic (TM) polarization will

\* E-mail: ar.mobini@iau-tnb.ac.ir

face in-plane dielectric function alike as graphite. Using this dielectric function, an all-angled waveguide in the scale of nanometer had been designed based on a triangular MWCNT array in our previous work<sup>[19]</sup>. As regards to the absorption properties occurred due to the dispersive band structure which had not been studied clearly up to now, especially in the area of infrared (IR) regime, we investigated the master piece response of PCs with two-dimensional (2D) MWCNT square arrays for designing advanced absorbers in the IR regimes. There are different technologies to design devices for detection and absorption applications. In our last work, we designed a quantum ring based detector for thermal detection<sup>[23]</sup>.

We present photonic band structure and scattering parameters of MWCNT based PCs for the TM polarization (electric field parallel to nanotube axis). In the next section we are going to elucidate the structural and numerical model used in simulations. Then we follow up the dispersive band structure, reflection, and absorption coefficient of structures with various lattice constants ( $a$ ) and proper filling factors ( $f$ ), and eventually, used the results for designating advanced IR absorber.

The finite-difference time-domain (FDTD) method, in which Maxwell's equations are solved on a computational grid had been used to calculate the optical response of 2D square array with lattice constant of  $a$  and filling ratio of  $f$ . The filling ratio is assumed to be the cross sectional area of MWCNT covered in the square unit cell. In other word, it is the percentage of  $\pi r^2/a^2$  in which  $r$  is the radius of the MWCNT and  $a$  is the lattice constant of the structure (Fig.1). We assumed that the vertical length of cylindrical rods of MWCNT material to be infinite. This is authentic as the length of rods is much more immense than their diameters<sup>[24,25]</sup>. In addition, the whole cylinders are fully covered with the MWCNTs material. It is also proved in Ref.[22] that the spaces among sheets would not cause significant changes on optic responses. For TM polarization, the dielectric function of MWCNT material comes up with only calculating the  $\epsilon_{\perp}$  part<sup>[19,25,26]</sup>. The equation below describes the dielectric function of TM polarized MWCNT that is modeled with multipole Drude-Lorentz dispersion as follows

$$\epsilon_{\perp}(\omega) = 1 - \frac{\omega_p^2}{\omega^2 + \frac{i\omega}{\tau}} + \sum_{m=1}^{M=7} \frac{\sigma_m^2}{\omega_m^2 + \omega^2 - i\omega\gamma_m}, \quad (1)$$

where the first term is the infinite response ( $\epsilon_{\infty}$ ) of the dielectric function. The second term is the Drude dispersion caused by the contribution of free electrons and the last term comprises Lorentz oscillators corresponding to inter-band transition.  $\omega_p$  specifies plasma frequency,  $\tau$  is the relaxation time of free electron,  $\omega_m$  shows the resonant frequency,  $\sigma_m$  is considered as oscillator strength, and  $\gamma_m$  is called for the decay rate of Lorentz term. Using Eq.(1) and the values in Ref.[26], both real and imaginary parts of the dielectric function are plotted in combination of reflection part in Fig.2(b). It is obvious

that there are two peaks in the imaginary part related to  $\sigma$  and  $\pi$  transitions (4.5 eV and 14.3 eV), corresponding to metallic characteristic of the structure<sup>[26]</sup>. There are also two valleys on the same energies in real part with negative values.

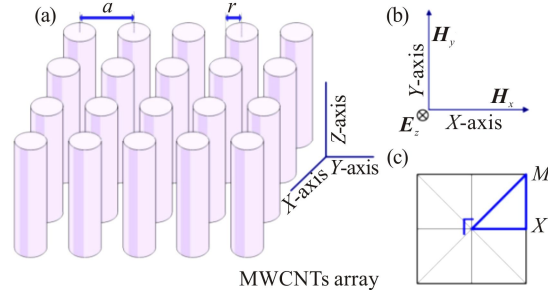


**Fig.1 (a) 2D MWCNTs' square array with lattice constant  $a$  and nanotube radius  $r$ ; (b) TM polarization; (c)  $\Gamma$ -X-M reciprocal lattice model**

For the PC consisting of a square array of 2D MWCNTs with the lattice constant of 15 nm, dispersive band structure and reflection coefficient have been calculated using COMSOL Multiphysics package and shown in Fig.2(a) and Fig.2(b), respectively. All the absorption and reflection coefficients are normalized to input power. The diameter of each nanotube is 119.71 nm, so the filling ratio would be equal to 50%. As seen in Fig.2(b), there are three main peaks in the reflection coefficient. Two of them are in the range around 5 eV and 15 eV ( $\sim 248$  nm and 83 nm), which are caused by the plasmonic behavior of the material as the energy transition of  $\pi \rightarrow \pi^*$  and  $\sigma \rightarrow \sigma^*$ , so they are named as metallic peaks. The one remaining is called the Bragg peak, which occurred around 45 eV ( $\sim 27.5$  nm). Also, these peaks are consistent with band structure plotted in Fig.2(a), in which there is no band in the mentioned photon energies. To be specific, when we observe a gap in the band structure diagram, it refers there would be a peak in the reflection coefficient on the same photon energies. Accordingly, there would be a valley in the same energies on the absorption response. Conforming the strength of the multiple scattering, complete or partial spectral gaps may occur, which leads to high absorption properties especially in our desired IR regime that had not been studied before. The absorption coefficient for this structure is calculated. As seen in Fig.2(c), there are three valleys almost around 5 eV, 15 eV and 45 eV, corresponding to three peaks in the reflection coefficient (Fig.2(b)). This means that when the reflection coefficient has its maximum value, the absorption coefficient decreases as promised. This happened because the incident light is reflected and cannot propagate through structure. In this way, between these created valleys in absorption coefficient, corresponding peaks occurred simultaneously, showing the maximum values of the absorption coefficient. Photon energies of the first and two peaks are fixed because their corresponding valleys have occurred in fixed energies caused by the metallic property, but the third peak is variable and can occur in

different wavelengths depending on the Bragg reflection peaks. Bragg peaks occurrence is the main difference between reflection responses of graphite and MWCNTs array, so the study of MWCNTs array is interesting and promising.

Therefore, due to intrinsic properties of reflection peaks, it is expected that for different arrays of MWCNTs, metallic peaks will appear in the same energies, but the Bragg peaks will differ, depending on the structure parameters, i.e., the lattice constant and the filling factor. For further realization, we calculated the band structure and reflection coefficient of MWCNTs array with the increased lattice constant of 30 nm and the same filling ratio of 50% (Fig.3). As seen in Fig.3(a), the full metallic band gaps occurred almost around 5 eV and 15 eV, the same as previous calculations, but the Bragg band gap shifted and behaved completely different in comparison. This fact can be also figured out in Fig.3(b), as the metallic peaks occurred in the same energies (almost around 5 eV and 15 eV) related to the metallic band gaps in Fig.3(a). But the Bragg peak has different trend and shifts to lower energies, almost in  $\sim 46$  nm, which can be seen as the third peak in reflection coefficient. With enlarging  $a$ , this band gap enters metallic region and has anti-crossing and finally will shift to our desired regime. The absorption coefficient of this structure is denoted in Fig.3(c). The first two valleys behave in the same manner with the previous structure, serving as the metallic response, although the next valley is fluctuated by the interaction of Bragg peak in the reflection coefficient.

Considering these facts, we investigated how the Bragg peak can occur in lower energies (larger wavelengths) especially in the IR regime ( $<2$  eV or 620 nm). As proved, the metallic band gaps occur above 2 eV, so they are far away from our desired regime and only the Bragg gaps will be effective in IR absorption. Furthermore, there is another interesting note that in lower energies ( $<2$  eV), both real and imaginary parts of dielectric function increase and lead to more absorption. So we expect that MWCNTs array with larger lattice constant could behave like an optical absorber in this regime.

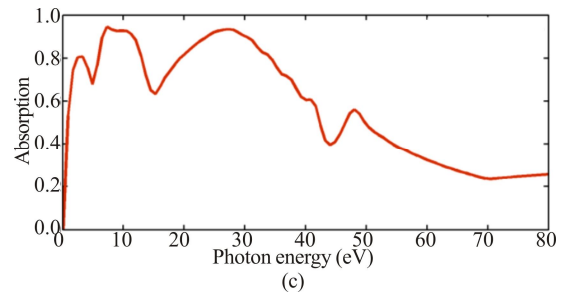
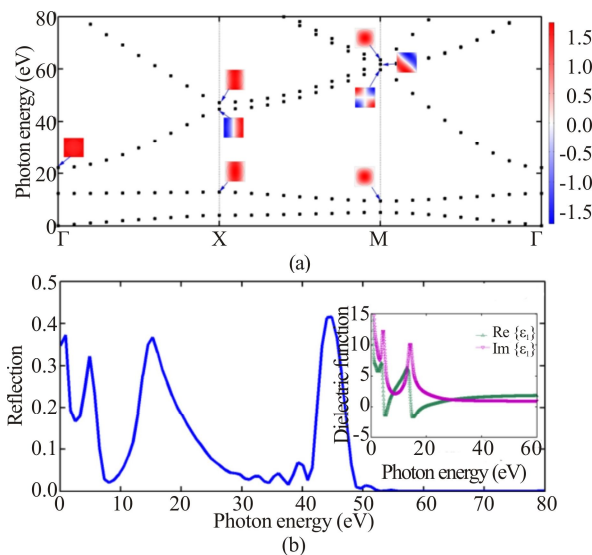


**Fig.2 Photonic responses of 10-row MWCNTs square arrays with  $a=15$  nm and  $f=50\%$ : (a) Disperse band structure; (b) Normalized reflectance; (c) Normalized absorbance**

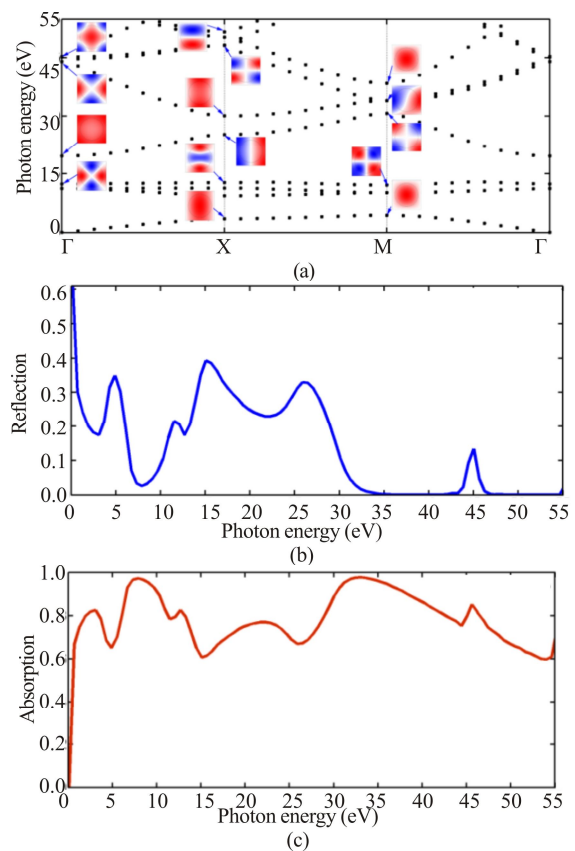


**Fig.3 Photonic responses of 10-row MWCNTs square arrays with  $a=30$  nm and  $f=50\%$ : (a) Disperse band structure; (b) Normalized reflectance; (c) Normalized absorbance**

In the following, we have increased the lattice constant to 600 nm. The photonic band structure and reflection coefficient of the array with  $a=600$  nm and  $f=5\%$  are calculated and plotted in Fig.4. There is a full Bragg gap almost around 0.5 eV (2.48  $\mu$ m) in the near infrared (NIR) regime. Also, there are two partial Bragg gaps about 2.1 eV and 2.45 eV photon energies that are far away from the IR regime and have not been considered. In addition, the absorption coefficient of this structure had been calculated and denoted in Fig.4(c). There are three valleys in about 1 eV ( $\sim 1.2$   $\mu$ m), 2.1 eV ( $\sim 0.6$   $\mu$ m) and 2.45 eV ( $\sim 0.5$   $\mu$ m) according to peaks in the reflection coefficient. The weak peak in the absorption coefficient has occurred

under 1 eV near the desired IR regime, but it is not strong enough. The other peak is about 1.8 eV ( $\sim 0.68 \mu\text{m}$ ), still far from IR regime. This peak location and amplitude can be manipulated with the Bragg peak achieved by increasing lattice constant.

So we will investigate the optical parameters of the array with the larger lattice constant in the following.

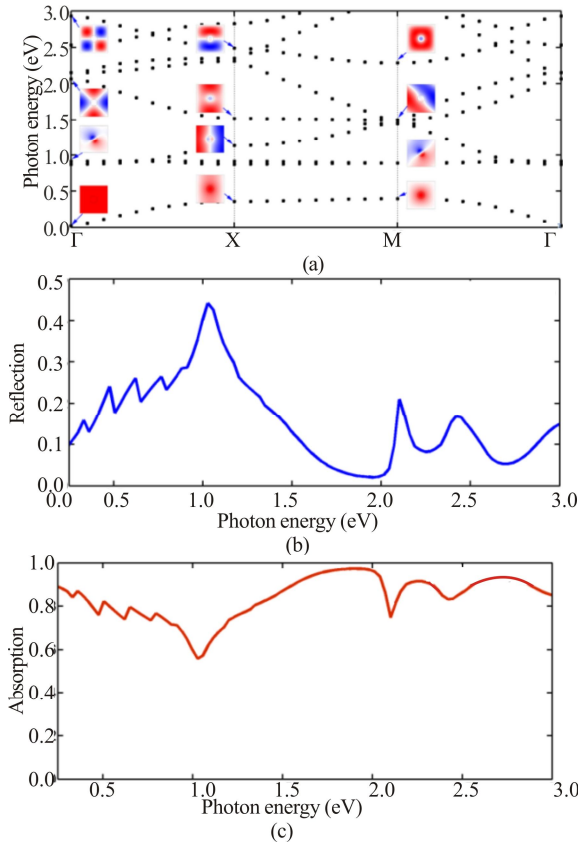
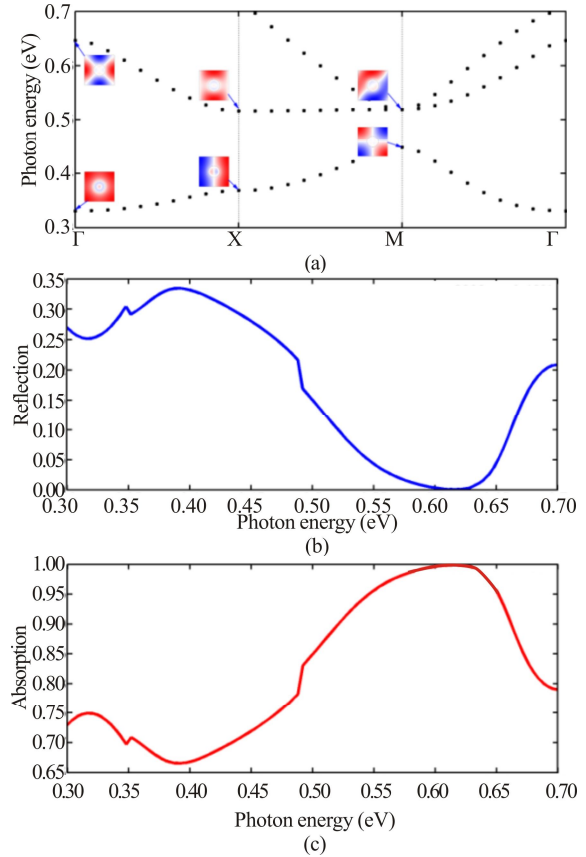


**Fig.4 Photonic responses of 10-row MWCNTs square arrays with  $a=600 \text{ nm}$  and  $f=5\%$ : (a) Disperse band structure; (b) Normalized reflectance; (c) Normalized absorbance**

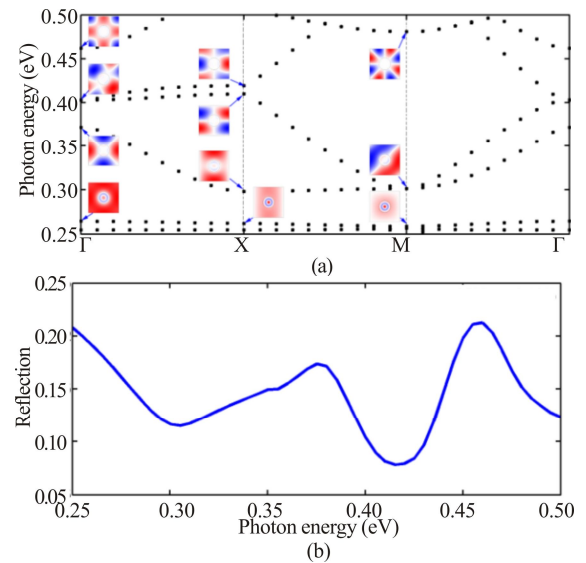
We increased the lattice constant to 2 000 nm. The related dispersive band structure of MWCNT PC with a lattice constant of  $a=2 \text{ 000 nm}$  was calculated and is shown in Fig.5(a). Also, the reflection and absorption responses of the structure were calculated and denoted in Fig.5(b) and Fig.5(c), respectively. There are two band gaps almost in the energies of 0.36 eV ( $\sim 3.5 \mu\text{m}$ ) and 0.66 eV ( $\sim 1.87 \mu\text{m}$ ) in the band structure. The corresponding peaks also appear in the reflection spectrum in the same energies. These fluctuations in the reflection coefficient affected the absorption spectrum and led to a peak for wavelengths between  $1.9 \mu\text{m}$  to  $2.14 \mu\text{m}$ . The curve gets the maximum at  $\lambda=2 \mu\text{m}$  with more than 99% absorption. This structure can be used in designing absorbers in the NIR regime.

Utilizing these results, we tried to achieve a good absorber in the mid infrared (MIR) regime, so we enhanced  $a$  to 3 500 nm. The photonic band structure, reflection,

and absorption coefficients were calculated and shown in Fig.6. There is a band gap of about 0.37 eV ( $\lambda=3.3 \mu\text{m}$ ) in the band structure with a corresponding peak in the reflection coefficient. As expected, there is a peak of  $3.5 \mu\text{m}$  in the MIR region in the absorption spectrum which is manipulated with Bragg peak.



**Fig.5 Photonic responses of 10-row MWCNTs square arrays with  $a=2 \text{ 000 nm}$  and  $f=12\%$ : (a) Disperse band structure; (b) Normalized reflectance; (c) Normalized absorbance**



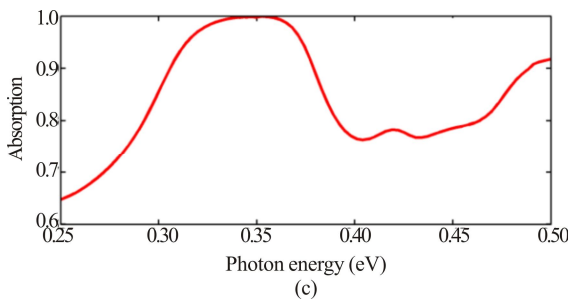


**Fig.6 Photonic responses of 10-row MWCNTs square arrays with  $a=3500$  nm and  $f=12\%$ : (a) Disperse band structure; (b) Normalized reflectance; (c) Normalized absorbance**

Towards optimizing structure, we investigated the structural parameters. The filling ratio can change scattering parameters in structure, so it can affect the absorption response. To achieve maximum absorption, we swept the filling factor from 4% to 70% for lattice constant of 2000 nm and 3500 nm. The corresponding absorption coefficients are calculated and shown in Fig.7(a) and Fig.7(b), respectively.

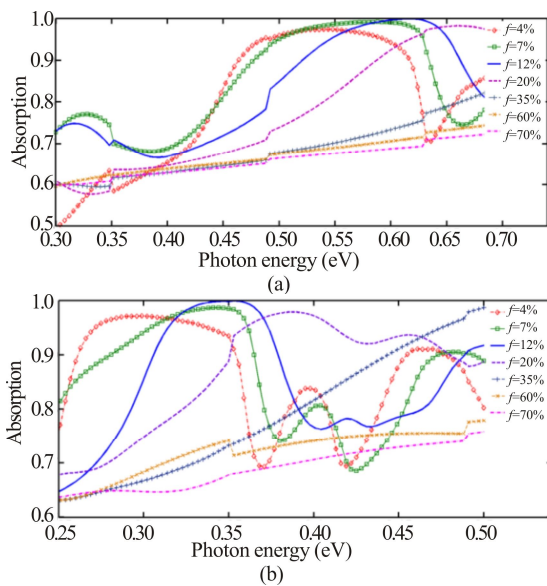


**Fig.7 10-row MWCNT array's normalized absorbance for (a)  $a=2000$  nm with different filling ratios and (b)  $a=3500$  nm with different filling ratios**

The absorption spectrum with  $a=2000$  nm has a peak around 0.55 eV ( $\sim 2.25$   $\mu\text{m}$ ) for  $f=4\%$ . As  $f$  increased to 7%, 12% and 20%, related peak in the absorption spectrum presented blue shift and moved to 0.6 eV, 0.61 eV, and 0.66 eV, respectively. As it is clear for wavelengths between 1.96  $\mu\text{m}$  and 2.13  $\mu\text{m}$ , the absorption is more than 99% and maximized at  $\lambda=2$   $\mu\text{m}$  with more than 99.99%. Thus that can be a good absorber used in designing applications in the NIR region.

In this way, the absorption spectrum with  $a=3500$  nm has a peak around 0.27 eV ( $\sim 4.5$   $\mu\text{m}$ ) for  $f=4\%$ . As  $f$  increased to 7%, 12% and 20%, related peak in the ab-

sorption spectrum presented blue shift and moved to 0.34 eV, 0.35 eV, and 0.38 eV, respectively. So the absorption is more than 99% for wavelengths between 3.4  $\mu\text{m}$  and 3.7  $\mu\text{m}$ , and maximized at  $\lambda=3.5$   $\mu\text{m}$  with more than 99.99%. Hence that can be a good absorber used in designing applications in the MIR region. Also, there is a blue shift in absorption coefficient when  $f$  increased. So the absorption spectrum can be tuned in the range from 0.27 eV to 0.38 eV ( $\lambda=4.6$ —3.3  $\mu\text{m}$ ) with changing  $f$ .

In summary, we used the FDTD method to analyze the absorption properties of 2D square arrays of MWCNT using the multipole Drude-Lorentz model inserted to the dispersive dielectric function of MWCNTs. We examined dispersive photonic band structure, reflection and absorption coefficient of proposed structures with a large lattice constant ( $> 600$  nm) and achieved high absorption (more than 99.9%) for the NIR regime with  $a=2000$  nm and  $f=12\%$ . Also for the MIR regime, we achieved a total absorber with 99.9% absorption. It is worth to note that the absorption spectrum peak can be tuned in the range of 0.27—0.38 eV ( $\lambda=4.59$ —3.26  $\mu\text{m}$ ) with a changing filling factor. These results will help engineers to design new devices, such as IR absorber and solar cells based on MWCNT PCs.

### Statements and Declarations

The authors declare that there are no conflicts of interest related to this article.

### References

- [1] IJIMA S. Helical microtubules of graphitic carbon[J]. Nature, 1991, 354(6348): 56-58.
- [2] WILKINSON T, BUTT H. Hybrid carbon nanotube-liquid crystal nanophotonic devices[M]// YAMASHITA S, SAITO Y, CHOI J H. Carbon nanotubes and graphene for photonic applications. Amsterdam: Elsevier, 2013: 319-350e.
- [3] YAMASHITA S, SAITO Y, CHOI J H. Carbon nanotubes and graphene for photonic applications[M]. Amsterdam: Elsevier, 2013.
- [4] ROUF S A, USMAN Z, MASOOD H T, et al. Synthesis and purification of carbon nanotubes[M]// Carbon nanotubes-redefining the world of electronics. London: IntechOpen, 2021.
- [5] DRESSELHAUS M S, DRESSELHAUS G, AVOURIS P H. Carbon nanotubes[M]. Berlin : Springer, 2001.
- [6] TIAN Y. Optical properties of single-walled carbon nanotubes and nanobuds[J]. Aalto University Publication, 2012.
- [7] WU Y, ZHAO X, SHANG Y, et al. Application-driven carbon nanotube functional materials[J]. ACS nano, 2021, 15(5): 7946-7974.

- [8] PENG L M, WANG S, ZHANG Z. Carbon nanotube-based photovoltaic and light-emitting diodes[M]//YAMASHITA S, SAITO Y, CHOI J H. Carbon nanotubes and graphene for photonic applications. Amsterdam: Elsevier, 2013: 298-318.
- [9] RAJAPUTRA S, MANGU R, CLORE P, et al. Multi-walled carbon nanotube arrays for gas sensing applications[J]. Nanotechnology, 2008, 19(34): 345502.
- [10] BUTT H, DAI Q, RAJESKHARAN R, et al. Plasmonic band gaps and waveguide effects in carbon nanotube arrays based metamaterials[J]. ACS nano, 2011, 5(11): 9138-9143.
- [11] GHEITAGHY A M, GHADERI A, VOLLEBREGT S, et al. Infrared absorbance of vertically-aligned multi-walled cnt forest as a function of synthesis temperature and time[J]. Materials research bulletin, 2020, 126: 110821.
- [12] JI Y Y, FAN F, XU S T, et al. Terahertz dielectric anisotropy enhancement in dual-frequency liquid crystal induced by carbon nanotubes[J]. Carbon, 2019, 152: 865-872.
- [13] MUNIYAPPA M, DODDAKUNCHE S P, GOWDA S G, et al. Carbon nanostructure based composites for environmental and energy applications[M]//Advances in nanocomposite materials for environmental and energy harvesting applications. Berlin: Springer, 2022: 35-74.
- [14] DVUZHILOVA Y V, DVUZHILOV I, BELONENKO M. Three-dimensional light bullets in an optically anisotropic photonic crystal with carbon nanotubes[J]. Bulletin of the Russian Academy of Sciences: physics, 2022, 86(1): 46-49.
- [15] MOHAMMADI M, FARAHMAND M, OLYAEE S, et al. An overview of all-optical memories based on periodic structures used in integrated optical circuits[J]. Silicon, 2022: 1-20.
- [16] PARANDIN F, HEIDARI F, RAHIMI Z, et al. Two-dimensional photonic crystal biosensors : a review[J]. Optics & laser technology, 2021, 144: 107397.
- [17] SUKHOIVANOV I A, GURYEV I V. Photonic crystals: physics and practical modeling[M]. Berlin: Springer, 2009.
- [18] KHANI S, HAYATI M. Optical biosensors using plasmonic and photonic crystal band-gap structures for the detection of basal cell cancer[J]. Scientific reports, 2022, 12(1): 1-19.
- [19] MOBINI A, AHMADI V. Nanoscale all-angle waveguide based on plasmon band effect in triangular array of mwents[J]. Journal of lightwave technology, 2013, 31(23): 3859-3864.
- [20] SHOJI S, SUZUKI H, ZACCARIA R P, et al. Optical polarizer made of uniaxially aligned short single-wall carbon nanotubes embedded in a polymer film[J]. Physical review B, 2008, 77(15): 153407.
- [21] CHEN Y C. Ultrafast optical switching properties of single-wall carbon nanotube polymer composites at 1.55  $\mu\text{m}$ [J]. Applied physics letters, 2002, 81(6): 975-977.
- [22] SHAMSOLLAHI Y, MORAVVEJ-FARSHI M K, EBNALI-HEIDARI M. Photonic crystals based on periodic arrays of mwents: modeling and simulation[J]. Journal of lightwave technology, 2013, 31(12): 1946-1953.
- [23] MOBINI A. Investigation on rashba spin-orbit interactions in two dimension quantum array for thermal imaging applications[J]. Journal of Optics, 2020, 22(8): 085001.
- [24] CHHOWALLA M. Growth process conditions of vertically aligned carbon nanotubes using plasma enhanced chemical vapor deposition[J]. Journal of applied physics, 2001, 90(10): 5308-5317.
- [25] CASIRAGHI C. Rayleigh imaging of graphene and graphene layers[J]. Nano letters, 2007, 7(9): 2711-2717.
- [26] LIDORIKIS E, FERRARI A C. Photonics with multiwall carbon nanotube arrays[J]. ACS nano, 2009, 3(5): 1238-1248.